Article

# Rapid and Convenient Potentiometric Method for Determining Fluorosulfate, a Byproduct of the Fumigant and Greenhouse Gas Sulfuryl Fluoride

Zhihao Chen, Chengjin Wang, and Joseph J Pignatello*

Read Online

ACCESS | Metrics & More | Article Recommendations | SI Supporting Information

**ABSTRACT:** A fluorosulfate ion $(FSO_3^-)$ is a hydrolysis product of sulfuryl fluoride $(SO_2F_2)$, which is widely used to fumigate buildings, soil, construction materials, and postharvest commodities, and is a potent greenhouse gas. It is a potential marker for biological exposure to $SO_2F_2$ and for monitoring the progress of reactions used to scrub $SO_2F_2$ from fumigation vent gases. Here, we report a simple and inexpensive potentiometric method for determining $FSO_3^-$ using a commercial nitrate-selective electrode and discuss its application. The method is suitable for solutions between 0.0025 mM and 660 mM $FSO_3^-$ at initial pH between 5 and 9. Halide interference depends on its molar ratio to $FSO_3^-$ and follows the sequence, $F^- < Cl^- < Br^- \ll I^-$. Halide interference can be eliminated by adding silver sulfate. Interference by bicarbonate can be eliminated by $H_2SO_4$ pretreatment, and interference by phosphate or pyrophosphate by $MgSO_4$ addition. Sulfate does not interfere, as it does in ion chromatography. Satisfactory method detection limits for $FSO_3^-$ in spiked aqueous extracts of 11 fruits were obtained. The method accurately quantified the yield of $FSO_3^-$ relative to that of $F^-$ in base hydrolysis of $SO_2F_2$. This study demonstrates that the developed method is highly selective, convenient, and sensitive and thus can be of great value in practice.
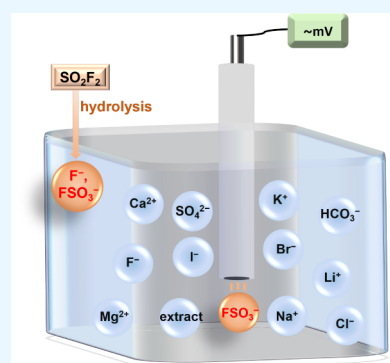
## 1. INTRODUCTION

Fluorosulfate $(FSO_3^-)$, the conjugate base of fluorosulfuric acid $(pK_a, -10)$, is a chemical intermediate in inorganic[1−4] and organic synthesis,[5−15] and is produced in certain reactions of interest in agricultural and environmental contexts.[16,17] A major source of $FSO_3^-$ is the decomposition of sulfuryl fluoride $(SO_2F_2)$, which is widely used to rid pests in buildings and structures, agricultural soils, and postharvest commodities in quarantine and preshipment operations.[18−26] Sulfuryl fluoride is increasingly used as a replacement fumigant for the ozone-depleting gas, methyl bromide. Foods treated with $SO_2F_2$ include wheat,[20] flours,[23] animal-based stored products,[27] cereals and cereal products, pulses and pulse products, dried fruits, tree nuts,[28] dried beef, gluten, and many others.[29] Spent fumigation gases of $SO_2F_2$ are generally vented to the atmosphere. Of concern is the greenhouse gas potential of $SO_2F_2$.[30,31] Atmospheric $SO_2F_2$ has a global warming potential 4780 times greater than carbon dioxide[32,33] and a lifetime of 36 ± 11 years.[24,25] The mole fraction of $SO_2F_2$ in the atmosphere grew by 5 ± 1% per year from 1978 to 2007, with estimated yearly emissions increasing from 0.6 Gg in 1978 to 1.9 Gg in 2007;[24,25] by 2019, global emissions had increased to 2.9 ± 0.4 Gg/yr.[24]

The potency of $SO_2F_2$ as a greenhouse gas has prompted investigative efforts to remove it from fumigation vent streams, such as solvent adsorption and dielectric barrier discharge plasma.[19,33] A potentially more convenient method is

scrubbing with aqueous hydroxide solution, in which $OH^-$ acts as a nucleophile to attack the central sulfur and displace the fluorine with generation of equimolar amounts of $FSO_3^-$ and $F^-$ (eq 1).

$$SO_2F_2 + 2OH^- \rightarrow FSO_3^- + F^- + H_2O \tag{1}$$
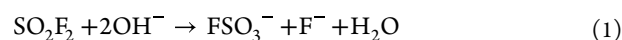
Sulfuryl fluoride is readily absorbed by tissues of fumigated products or animals,[23] where it can undergo nucleophilic and hydrolytic reactions leading to sulfate, fluoride, and fluorosulfate. Whereas $SO_2F_2$ itself is acutely toxic to fish, as well as to humans at high inhalation exposure,[34] the chronic neurotoxicity and other chronic toxicities of $SO_2F_2$ have been attributed to its breakdown products.[34,35] Fluoride and sulfate were found in a variety of fumigated foodstuffs including beef.[21] Fluorosulfate was identified in the urine and blood of rats exposed to $SO_2F_2$.[34] Sulfuryl fluoride has also been used in click chemistry to convert alcohols and amines to fluorosulfonate derivatives;[8−11] the fluorosulfonate group is then removed by base hydrolysis, producing $FSO_3^-$.[12−15] Metal fluorosulfates (such as $Li^+$) have been proposed for use

as electrolytes in batteries.[36] Lastly, $FSO_3^-$ is found naturally in the mineral Reederite-(Y) from Mont-Saint-Hilaire.[17] Fluorosulfate can be regarded at this time as persistent and mobile in the environment since it is stable to hydrolysis in water at ordinary pH[37,38] and only weakly coordinates to metal cations[38−40] and mineral surfaces.[17] While its toxicity is unknown, one study noted that $FSO_3^-$ inhibits crucial metabolic enzymes including acetylcholinesterase, butyrylcholinesterase, sulfatase, and glutathione *S*-transferase.[41] The potential toxicity of $FSO_3^-$ stresses the need for analytical methods for its determination.

A rapid and convenient method for $FSO_3^-$ would assist investigators in monitoring the decomposition of $SO_2F_2$ in fumigation applications, its presence in fumigated foodstuffs, and as an aid in chemical investigations where $FSO_3^-$ is a byproduct. However, rapid and convenient analytical methods for $FSO_3^-$ are lacking. So far, the only methods reported are based on ion chromatographic (IC) separation.[19,42] However, we find that the peaks for $FSO_3^-$ and $SO_4^{2-}$ in the ion chromatogram are difficult to separate (i.e., they have nearly the same retention time; vide infra). Sulfate is a natural component of water and tissues and is often coproduced in reactions involving $SO_2F_2$ (eqs 1 and 2).[21,34] Therefore, due to the interference of sulfate, IC is not a good analytical tool for $FSO_3^-$. Moreover, IC equipment is expensive and unsuitable for on-site use.

$$FSO_3^- + 2OH^- \rightarrow SO_4^{2-} + F^- + H_2O \quad (2)$$
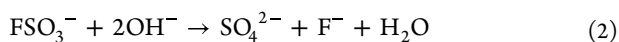
Potentiometric analysis is rapid and convenient and requires only inexpensive equipment.[43] We reasoned that a particular commercial nitrate-selective electrode might be workable for $FSO_3^-$ analysis, since the perchlorate ion $(ClO_4^-)$, which is isoelectronic and structurally similar to $FSO_3^-$, was claimed by the supplier to strongly interfere with nitrate analysis. Our prediction turned out to be correct; in fact, the electrode is more sensitive to fluorosulfate than nitrate for which it was designed. The main objectives of this study were to 1) test electrode selectivity in the presence of potentially interfering ions, 2) validate the method in a known reaction, namely, alkaline hydrolysis of $SO_2F_2$ (eq 1) and 3) test the method for determination of $FSO_3^-$ in tissues of fumigated food products.

## 2. EXPERIMENTAL SECTION

**2.1. Chemicals.** All chemicals were of analytical grade or higher purity and used as received unless stated. Potassium fluorosulfate $(KFSO_3, 99.5\%)$, potassium chloride (KCl, 99.0%), lithium chloride (LiCl, 99.7%), magnesium chloride hexahydrate $(MgCl_2 \cdot 6H_2O, 99\%)$, sodium bromide (NaBr, 99.5%), potassium iodide (KI, 99+%), sulfuric acid $(H_2SO_4,$ 95.0−98.0 w/w % Plus grade), and potassium hydroxide (KOH, 99.98%) were purchased from Thermo Fisher Scientific. Potassium fluorosulfate was stored in a desiccator. Hydrogen peroxide solution ($\geq$30%), sodium pyrophosphate decahydrate $(Na_4P_2O_7 \cdot 8H_2O, \geq 99\%)$, calcium chloride dihydrate $(CaCl_2 \cdot 2H_2O, 99\%)$, sodium perchlorate $(NaClO_4,$ 98%), potassium bicarbonate $(KHCO_3, 99.7\%)$, phosphorus pentoxide $(P_2O_5, \geq 99\%)$ and magnesium sulfate $(MgSO_4)$ were obtained from Sigma-Aldrich, US. A cylinder of $SO_2F_2$ was obtained gratis from Douglas Products. Potassium fluoride standard solution of 1000 mg-F/L was purchased from Cole-Parmer and stored at 4 °C. Diluted KOH and $H_2SO_4$ solutions

were used for pH adjustment; HCl, $HNO_3$, and $HClO_4$ were avoided because their anions interfere (see below).

To determine whether the purchased $KFSO_3$ contained absorbed water, samples were either oven-dried at 105 °C or placed in a desiccator containing a bed of anhydrous $CaCO_3$ (with <2% $CoCl_2$ as a colorimetric indicator) or phosphorus pentoxide $(P_2O_5)$ desiccant. Oven drying resulted in continuous mass loss and evidence of sublimation and/or decomposition (Figure S1 and Text S1). Desiccation resulted in the leveling-off of mass loss corresponding to 0.54% $(CaCO_3)$ or 0.18% $(P_2O_5)$ moisture content of the original commercial product (Text S1, Table S1). We made no correction for water content of the purchased $KFSO_3$ when making standard solutions.

**2.2. Measurement of $FSO_3^-$ and $F^-$ by Potentiometric and IC Methods.** A commercial glass nitrate-selective combination electrode (Cole-Parmer, # EW-27502−31, US) connected to a pH/ion analyzer (Corning 350, US) was used to quantify fluorosulfate. The reference electrode (Ag/AgCl (3 M KCl)) was a double junction electrode, of which the inner compartment is filled with KCl solution and the outer compartment with 0.1 M $(NH_4)_2SO_4$ solution. The nitrate ion exchanger is contained within a gelled, organophilic electrode membrane. When the electrode is inserted into a solution, ion exchange will take place between the membrane and specific ions, resulting in a redox potential difference obeying the Nikolsky-Eisenman equation (eq 3), a generalization of the Nernst equation,[44−46]

$$E = E^0 + 2.303(RT/z_iF)\log\left(a_i + \sum_{j \neq i} K_{ij}a_j^{z_i/z_j}\right) \quad (3)$$

where $E$ is the measured electrode potential; $E^0$ is constant potential determined by the electrode and background electrolyte; $R$ is the gas constant (8.314 J/K/mol); $T$ is the absolute temperature (K); $z_i$ is the charge number of the primary ion $(FSO_3^-)$; $F$ is the Faraday constant (96 487 C/mol); $a_i$ is the activity of freely dissolved $FSO_3^-$; $a_j$ is the activity of interfering ion j; $K_{ij}$ is the potentiometric selectivity coefficient (SC) for ion j with respect to $FSO_3^-$; and $z_j$ is the charge number of ion j. Here, activity was assumed equal to the ion concentration. In a background of high and constant ionic strength (IS), eq 3 is influenced only by ions that the electrode is sensitive to. It is the ion activity change that determines the obtained potential values and no obvious electrolysis takes place at the electrode membrane.[47] Theoretically, the electrode response is proportional to the log of the $FSO_3^-$ activity with a slope of 59 mV/decade at room temperature. The background ionic strength (IS) of the samples was controlled at 0.12 M according to the manufacturer's protocol for the electrode by adding an ionic strength adjuster (ISA, 2.0 M $(NH_4)_2SO_4$, pH 5.5) to sample at the volume ratio of 1:50. With slow and continuous stirring, the electrode response became stable within 2−5 min near the detection limit for $FSO_3^-$, but within 1 min at higher concentrations. The solution pH mentioned below for $FSO_3^-$ analysis corresponds to the value prior to ISA addition. Based on our experience, with frequent use, the electrode should last for one year if used and stored according to directions, indicating the low-cost of the analysis.

Fluoride was measured using a different, fluoride-selective glass combination electrode (Cole-Parmer, # EW 27502−19, US). Sample solutions were prepared and adjusted to pH 5.3 with acetate buffer according to the supplier's protocol.

Fluoride calibration curves were constructed based on the purchased standard solution (1000 mg-F/L).

The electrode method was compared against an ion chromatographic method (Metrohm 930 Compact IC Flex, Switzerland) employing a Metrosep A Supp 5−150/4.0 (poly(vinyl alcohol) with quaternary ammonium groups), which is widely used in IC. The mobile phase consisted of 3.2 mM $Na_2CO_3$ and 1.0 mM $NaHCO_3$ at a flow rate of 0.8 mL/min.

**2.3. Effects of pH and Interfering Ions.** The measured electrode potential can be sensitive to pH,[43,48,49] as well as certain ions besides $FSO_3^-$. Calibration curves were constructed at different pH values of 3.0, 5.0, 7.0, 9.0, and 11.0 of the samples adjusted prior to combining with the ISA. Samples with different concentrations of potentially interfering ions were adjusted to the desired pH prior to combining with the ISA.

**2.4. Food Tissue Extraction and Analysis.** The fluorosulfate ion may be generated in foods that have been fumigated with $SO_2F_2$.[23,28] To determine whether the proposed potentiometric method is suitable for determining $FSO_3^-$ residuals in food tissues, 12 foods were selected for analysis including broccoli, cucumber, sweet onion, sweet potato, strawberries, apple, carrot, yellow squash, blueberries, cauliflower, kiwi, and dried dog food. The raw foods were first chopped and blended. Then, except for the dog food, the food cells were lysed by subjecting the blended material to three freeze−thaw cycles (about 5 min each cycle) in liquid nitrogen to rupture cells.[50,51] The lysed tissues were further ground in a mortar and 2.5 g of each tissue were transferred to a small sealable flask with a desired volume of water. The flasks were heated in an oven at 65 °C for 24 h and then sonicated for 1 h to ensure that cellular components were completely released. After centrifugation at 6000 rpm for 15 min, the collected aqueous supernatant was filtered through a 0.45 μm membrane prior to addition of a known amount of $FSO_3^-$.

It was assumed that the extraction protocol efficiently extracted $FSO_3^-$. To verify this, raw food samples were directly spiked with $FSO_3^-$ and then processed by the extraction protocol. The recovery of $FSO_3^-$ was 91−103% (Text S2 and Table S2). As shown in Figure S2, all extracts of 10 (g tissue)/(L water) showed absorbance from 200 to 400 nm, indicating the presence of soluble organic or inorganic substances lysed from cells.

**2.5. Determination of $FSO_3^-$ and $F^-$ Produced by Base Hydrolysis of $SO_2F_2$.** To validate the proposed method, we measured $FSO_3^-$ and $F^-$ formed simultaneously during base ($OH^-$) hydrolysis of $SO_2F_2$. This reaction is known to produce $FSO_3^-$ and $F^-$ in an equimolar yield (eq 1).[52] The reactions were performed in a brown glass bottle (Microsolv Technology Corporation, US) sealed by a cap with a PTFE-lined silicone rubber septum. The liquid phase (100 mL) consisted of NaOH solution at pH 11.6 or 12.5 and the headspace volume was 25 mL. A stir rate of 700 rpm was used, which caused a vortex reaching to the 1/3 level of the flask. Sulfuryl fluoride (4 mL, room temperature) was transferred from its gas cylinder to the bottle via a Tedlar Sample Bag (SKC Co., Ltd.), which was flushed 3−4 times, and a gastight syringe. A second syringe with a long needle was used to withdraw liquid samples (2.5 mL) at fixed intervals. The samples were supplemented with 50 μL of acetic acid, which reduced the pH to 5.3 and stopped hydrolysis.[52] Then, aliquots were diluted 5-fold and analyzed for $F^-$ and $FSO_3^-$ separately.

**2.6. Data Analysis and Limit of Detection.** Deviation analysis was used to evaluate the effect of different interfering substances (ions, food extracts) on the measurement. The deviation percentage error ($\alpha$) is given by eq 4:

$$\alpha = \left| \frac{c_i - c_0}{c_0} \right| \times 100\% \tag{4}$$

where $c_0$ and $c_i$ represent the concentration obtained by the proposed potentiometric method without and with interfering substance, respectively. According to the Nikolsky-Eisenman principle,[44,46] $c_0$ corresponds to $a_i$ while $c_i$ is the sum of ($a_i + K_{ij}a_j$) in eq 3. The $\alpha$ is related to the selectivity coefficient by $K_{ij} = \alpha c_0/a_j$ (eq 3). We choose $\alpha$ here to clearly show the interference. To minimize the artifact of electrode response drift, measurements on samples with and without interfering ions taken at each reaction time were made immediately following one another. We considered $\alpha$ values of ≤10% to represent no significant effect of interfering matter.[53]

The limit of detection (LOD) is defined as the lowest detectable concentration of an analyte and is given by, LOD = $3.3 \times SD/S$, where SD is the standard deviation of the $y$-intercept and $S$ is the slope of the regression line.

## 3. RESULTS AND DISCUSSION

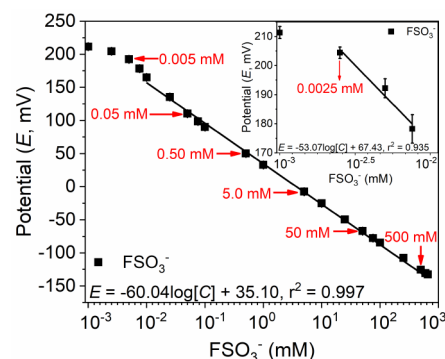**3.1. Construction of Calibration Curves and the Effect of pH.** Figure 1 shows a calibration curve constructed from



**Figure 1.** Calibration curve for $FSO_3^-$ solutions with the ion-selective electrode. The solution pH was ∼6.5 prior to mixing with the ISA. Linear fitting curves are shown between 0.0075 mM and 500 mM and between 0.0025 mM and 0.0075 mM (inset).

serial dilution of a stock solution of $KFSO_3$ at 660 mM (65.4 g/L $FSO_3^-$, close to the limit of solubility) adjusted to pH 6.5 with KOH. It was divided into two linear regions, a common practice with selective electrodes.[49,54,55] Between 0.0075 mM and 660 mM, the slope is −60.85 mV/decade, which is close to the theoretical slope of the Nikolsky-Eisenman equation (eq 3), and the $r^2$ value is 0.997. Between 0.0025 mM and 0.0075 mM, the slope (−53.07 mV/decade) deviates from theoretical, and the fit is poorer ($r^2 = 0.935$) (Figure 1, inset). We calculate the LOD to be 0.0007 mM and the limit of quantification to be $3.3 \times$ LOD, or approximately 0.0023 mM (230 μg/L).

The $FSO_3^-$ and $NO_3^-$ calibration curves are compared in Figure S3. The $FSO_3^-$ curve is slightly steeper than the $NO_3^-$ curve (slope, −61.72 vs −57.22), but both are close to the theoretical slope. More importantly, $NO_3^-$ gives an LOD (0.009 mM) about 10 times greater than the LOD for $FSO_3^-$.

This means the nitrate-selective electrode is more selective for $FSO_3^-$ than it is for $NO_3^-$.

The potentiometric response may depend on the pH of the sample before it is combined with the ISA due to the high mobility of hydrogen and hydroxide ions which will interfere the liquid-junction potential of the electrode.[43,45,48,56] Confirming this (Figure 2), the slope of the fitting line ranges
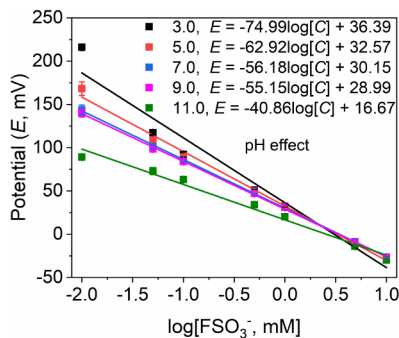


**Figure 2.** Calibration curves of $FSO_3^-$ at different solution pH values (3.0–11.0) prior to mixing with the ISA. The pH and corresponding $r^2$ values are 3.0 (0.95), 5.0 (0.99), 7.0 (1.00), 9.0 (1.00) and 11.0 (0.98).

from −74.99 mV/decade at pH 3.0 to −40.86 mV/decade at pH 11.0. At the extreme pH values of 3.0 and 11.0, the fits are noticeably poorer, and the slopes deviate substantially from the theoretical value of −59 mV/decade compared to the corresponding fits and values at pH 5, 7, and 9. We conclude that the acceptable pH range of the sample is 5.0–9.0, and for the best results we recommend that the calibration pH should be close to the expected sample pH, or else the samples should be neutralized with KOH or $H_2SO_4$ before adding the ISA.

**3.2. Potential Interferences.** We tested the effects on electrode response of some ions that may coexist with $FSO_3^-$ in applications, including halides, selected oxoanions, and selected metal ions. The results are shown in Figures 3, 4, S4,

and S5. We considered $\alpha$ within ±10% to indicate non-interference (eq 4).

*3.2.1. Effects of Halide Ions.* Fluoride is a potential interferant, as hydrolysis of both $SO_2F_2$ and $FSO_3^-$ gives $F^-$ as a product. Figure 3a shows that $F^-$ does not interfere with $FSO_3^-$ determination except at very low $FSO_3^-$ and very high $F^-$ such that $[F^-]$ is at least 1000 times greater than $[FSO_3^-]$. Chloride is ubiquitous in environmental waters and tissues.[57] Chloride added as KCl does not interfere except at very low $FSO_3^-$ and very high $Cl^-$ such that $[Cl^-]$ is at least 100 times $[FSO_3^-]$ (Figure 3b). The chloride counterion, $Ca^{2+}$, $Mg^{2+}$, or $Li^+$, has no effect (Figure S4).

Bromide added as NaBr does not interfere until $[Br^-]$ exceeds 20–100 times $[FSO_3^-]$ (Figure 3c). Iodide as KI strongly interferes if $[I^-]$ is more than twice the $[FSO_3^-]$ (Figure 3d). In summary, interference by halides follows the order, $F^- < Cl^- < Br^- \ll I^-$. According to the supplier of the electrode, interference by $Cl^-$, $Br^-$, and $I^-$ of nitrate analysis can be mitigated by adding silver sulfate to the solution. This was verified in the case of fluorosulfate (0.05 mM) for chloride (100 and 500 mM).

*3.2.2. Effects of Oxoanions.* Oxoanions of potential interest as potential interferents include nitrate, perchlorate, bicarbonate, sulfate, phosphate, and pyrophosphate. These ions may be present naturally in water samples or tissues, and their salts are commonly used as buffers or background electrolytes in chemical studies. Sulfate also is a recognized product of $FSO_3^-$ and $SO_2F_2$ hydrolysis.[37,38] The ISA introduces 0.04 M sulfate to all samples after mixing.

Despite being designed specifically for $NO_3^-$, the electrode is less sensitive to $NO_3^-$ than $FSO_3^-$ analysis, and $NO_3^-$ added in equivalent concentration to $FSO_3^-$ has no interference based on their separate potential response as shown in Figure S3. For example, at a potential of 196 mV, the concentration of $NO_3^-$ (2.6 mM) is 52 times that of $FSO_3^-$ (0.05 mM), while at 104 mV, the concentration of $NO_3^-$ (89.1 mM) is 63 times that of $FSO_3^-$ (1.41 mM). This means that $NO_3^-$ would have
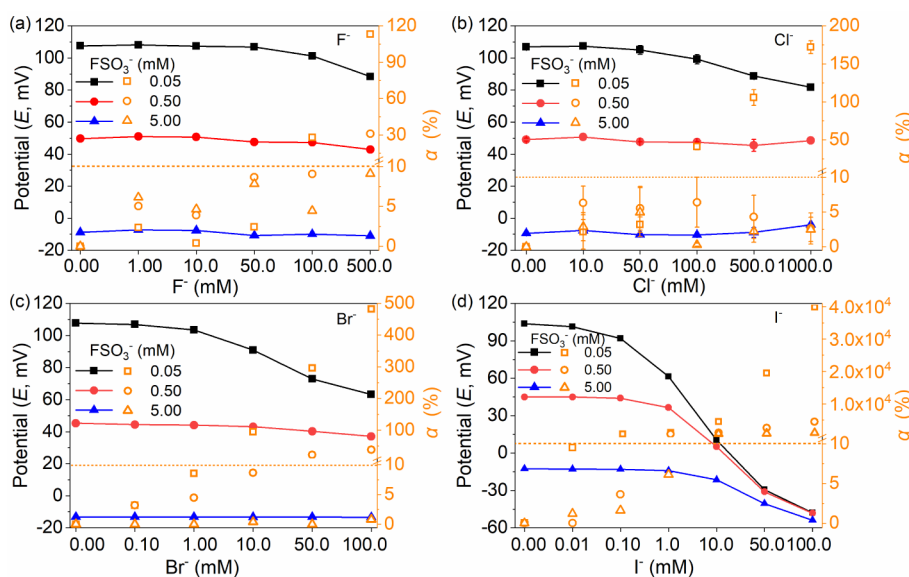


**Figure 3.** Effect of different concentrations of halide ions on the potentiometric response of 0.05 mM, 0.50 mM, and 5.00 mM $FSO_3^-$. The solid symbols refer to the left axis while the open symbols refer to the right axis. The dotted lines represent 10% error (eq 4). Break on $y$ axis in (a−d) ranges from 10.5 to 10.501.
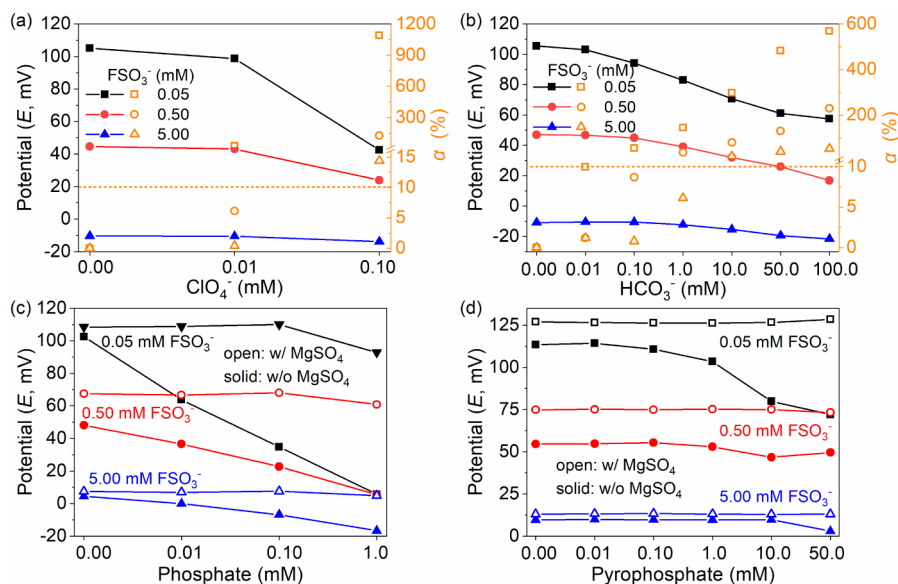
**Figure 4.** Effects of some common oxoanions on the potentiometric response of 0.05 mM, 0.50 mM, and 5.00 mM $FSO_3^-$: (a) perchlorate at pH 6.8 prior to mixing with ISA; (b) bicarbonate at pH 8.2; (c) phosphate at pH 7.4; (d) pyrophosphate at pH 6.5. For (a,b), the solid symbols refer to the left axis while the open symbols refer to the right axis. Dotted lines represent 10% error (eq 4). For (c,d), open and solid symbols represent with or without addition of 10 mM $MgSO_4$, respectively, and the $\alpha$ values are shown in Table S3.

to be much higher in concentration than $FSO_3^-$ for them to reach the same response intensity.

Perchlorate is known to interfere with $NO_3^-$ determination by this electrode, so it was not surprising to find that $ClO_4^-$ strongly interferes with $FSO_3^-$ determination, starting at concentrations as low as 20% that of $FSO_3^-$ (Figure 4a). (Bi)carbonate at pH 8.2 begins to interfere when its concentration reaches only double that of $FSO_3^-$ (Figure 4b). However, bicarbonate interference can be removed by prior acidification of the sample with sulfuric acid followed by gas sparging. Sulfate does not interfere at concentrations as high as 40 mM which is obtained anyway by adding the ISA. Phosphate at pH 7.4 strongly interferes even at 0.01 mM, but phosphate interference can be mitigated by addition of $MgSO_4$ which induces its precipitation after mixing with the ISA, presumably as $NH_4MgPO_4$ (Figure 4c).[58,59] The electrode response to $FSO_3^-$ is less sensitive to pyrophosphate interference at pH 6.5 than to phosphate interference at pH 7.4. Similar to phosphate, pyrophosphate interference can be eliminated by addition of $MgSO_4$ (Figure 4d). The electrode potentials in response to $FSO_3^-$ were higher with than without $MgSO_4$, which means that a separate calibration curve is needed if $MgSO_4$ is added to mitigate interference by phosphate or pyrophosphate (Table S3).

A strategy we are investigating to remove $SO_2F_2$ from fumigation vent streams is hydrogen peroxide ($H_2O_2$)-assisted alkaline defluorination.[60] In this reaction, $H_2O_2$ (as $HO_2^-$) displaces both F atoms as $F^-$ in successive steps and generates the oxo-anions, peroxymonosulfate (PMS; $HOOSO_3^-$), and peroxydisulfate (PDS; $^-O_3SOOSO_3^-$) as minor byproducts. We therefore tested for potential interference by PMS and PDS (Figure S5). The monoanion PMS began to interfere when its concentration exceeded 20-times that of $FSO_3^-$. The dianion PDS began to interfere when its concentration exceeded only twice that of $FSO_3^-$. As expected, $H_2O_2$ did not interfere (data not shown).

Given the results in Figures 3, 4, S4, and S5, the reader is alerted that oxoanions besides those tested here may interfere.

**3.3. Validation and Practical Application.** *3.3.1. Comparison with Ion Chromatography.* We attempted to compare the electrode method with an ion chromatographic (IC) method for $FSO_3^-$ analysis. Nie et al.[19] used a strong base quaternary ammonium anion exchange resin column to detect $FSO_3^-$ as a base hydrolysis product of $SO_2F_2$. They assigned the peak eluting at about 11.4 min to $SO_4^{2-}$ and the peak at about 13.7 min to $FSO_3^-$, an elution order that seems counterintuitive due to the difference in charge. Few details were given, and the authors did not attempt to quantify yields by IC. However, using a similar column from the same supplier and the same eluent we found it was not possible to separate the peaks for $SO_4^{2-}$ and $FSO_3^-$, in each case appearing at about 13.3 min. Details are provided in Text S3 and Figure 5. The source of the discrepancy between our results and those of Nie et al.[19] is unclear. In any case, it appears that $SO_4^{2-}$ has the potential to significantly interfere with $FSO_3^-$ determination by IC.

*3.3.2. Validation against a Second Product in Known Yield: The Case of Base Hydrolysis of $SO_2F_2$.* The purpose of this set of experiments was to validate the electrode method by employing it in a reaction that generates $FSO_3^-$ in a known ratio to a second product that can be determined independently. The reaction is strong base hydrolysis of $SO_2F_2$, which is reported to generate $F^-$ and $FSO_3^-$ in a ratio slightly greater than 1 (eq 1). The ratio is not equal to 1 because $FSO_3^-$ undergoes further slow hydrolysis to sulfate according to eq 2.[52] Simultaneous measurement of $FSO_3^-$ using the proposed nitrate-selective electrode and $F^-$ using the fluoride-selective electrode was performed during base hydrolysis of $SO_2F_2$ at pH 11.6 or 12.5 (Figure 6). The molar ratio of $F^-$ to $FSO_3^-$ was found to be $\sim$1.1, slightly greater than the 1:1 stoichiometry of eq 1, and as anticipated. Thus, the developed method for $FSO_3^-$ is validated against a second product in known yield. Furthermore, this reaction constitutes a realistic application of the method.

*3.3.3. Determination of Fluorosulfate in Food Tissues.* The need for analytical tools to determine $FSO_3^-$ residuals in
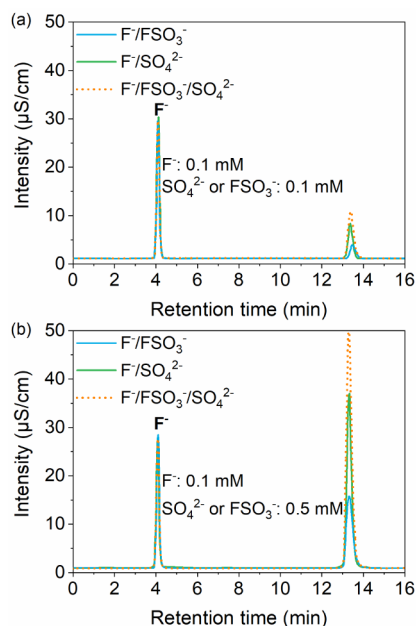
**Figure 5.** Ion chromatogram results for mixtures of $F^-/SO_4^{2-}$, $F^-/FSO_3^-$ and $F^-/FSO_3^-/SO_4^{2-}$. Concentrations respective $FSO_3^-$ and $SO_4^{2-}$ are 0.10 mM in (a) and 0.5 mM in (b). For (a), areas of $F^-$ are 9.106, 9.319, and 9.159, and the corresponding peak areas at 13.4 min are 9.989, 5.545, and 15.278. For (b), areas of $F^-$ are 9.505, 9.370, and 9.369, and the corresponding peak areas at 13.3 min are 1.960, 1.008, and 3.103. $F^-$ of 0.10 mM was used as an internal standard for all samples.
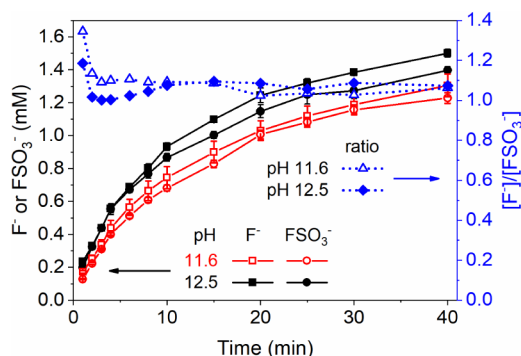


**Figure 6.** Evolution of $F^-$ and $FSO_3^-$ (left) and their ratio (right, blue curves) during base hydrolysis of $SO_2F_2$ at initial pH values of 11.6 and 12.5 in a sealed vial. Final pH values were 11.1 and 12.3, respectively. Injected $SO_2F_2$ volume is 4.0 mL, which corresponds theoretically to 1.6 mM $SO_2F_2$ in the liquid phase. The rate is faster at pH 12.5 because it is first order in hydroxide concentration.

food tissues will likely increase as $SO_2F_2$ use in the fumigation of foods expands.[21,28] $SO_2F_2$ is absorbed by protein-rich stored products.[61] To validate the use of the developed method under realistic conditions, $FSO_3^-$ was spiked into the aqueous food extracts of 12 different commercially available foods including 11 vegetables and a dog food product. Recovery of $FSO_3^-$ directly injected to vegetable tissue just prior to workup prior to workup was quantitative (Section 2).

Measured electrode potentials in the presence of different concentrations of tissue extracts are listed in Table S3, and the corresponding amounts of $FSO_3^-$ (g) per gram tissue are listed in Table S4. The corresponding deviations ($\alpha$) are shown in

Figure 7. Generally, $\alpha$ decreases with increasing concentration of $FSO_3^-$ in tissue extract (Figure 7).
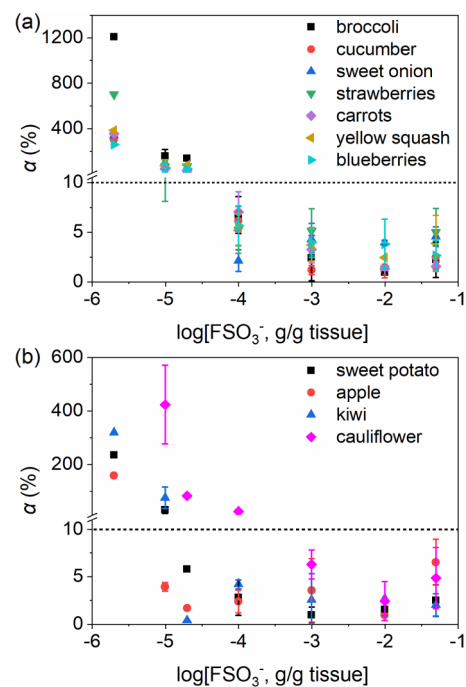


**Figure 7.** Electrode response deviation ($\alpha$, 100%) from the control with an increasing amount of $FSO_3^-$ in various fresh food tissues of (a) broccoli, cucumber, sweet onion, strawberries, carrots, yellow squash, and blueberries; (b) sweet potato, apple, kiwi, and cauliflower. The short dot line is where the deviation value is 10% (eq 4), above which this potentiometric method is considered as inappropriate.

The substances in the specific food extract have a significant effect on the $FSO_3^-$ method detection limit. For broccoli, cucumber, sweet onion, strawberries, carrots, yellow squash, and blueberries, $\alpha$ remained below 10% above $4.95 \times 10^{-5}$ (g $FSO_3^-$)/(g tissue) (Figure 7a). The method detection limit for these products thus lies in the range of $1.98-4.95 \times 10^{-5}$ (g $FSO_3^-$)/(g tissue). For sweet potato, apple, and kiwi, the method detection limit lies in the range of $0.99-4.95 \times 10^{-5}$ (g $FSO_3^-$)/(g tissue) (Figure 7b). Cauliflower extract had a higher method detection limit of $0.99-4.95 \times 10^{-4}$ (g $FSO_3^-$)/(g tissue) (Figure 7a). Therefore, depending on the food, the detection limit for $FSO_3^-$ may vary from $0.99 \times 10^{-5}$ (g $FSO_3^-$)/(g tissue) to $4.95 \times 10^{-4}$ (g $FSO_3^-$)/(g tissue). The method detection limit for $FSO_3^-$ in dog food is $0.50-4.95 \times 10^{-1}$ (g $FSO_3^-$)/(g tissue), which is much higher compared to the other foods (Figure 7 and Tables S3 and S4). The higher detection limit for dog food is probably because dog food has more soluble organic material and contains added ingredients.[62] This is consistent with dog food extract having the strongest absorbance in the UV–visible region among the tissue extracts (Figure S2). It is best to prepare calibration solutions at the same pH as that of the food tissue extract. Overall, the developed method can be used for $FSO_3^-$ determination in many food tissues.

## 4. CONCLUSIONS

We report a potentiometric method for quantification of $FSO_3^-$, a residual found in $SO_2F_2$-fumigated commodities and a byproduct of $SO_2F_2$ removal technologies, adopting a

commercially available nitrate-selective electrode. The electrode is more sensitive to $FSO_3^-$ than to $NO_3^-$ in practice. It has a quantifiable range of 0.0025−660 mM $FSO_3^-$. Unlike ion chromatography, sulfate does not interfere. Selectivity for $FSO_3^-$ is satisfactory in the presence of most halides, many oxyanions, and food tissue extracts. Although some buffer ions (bicarbonate, phosphate, and pyrophosphate) interfere, their interference can be mitigated by addition of other reagents (sulfuric acid for bicarbonate; magnesium sulfate for phosphate and pyrophosphate). The method appears to be suitable for analyzing $FSO_3^-$ in many produce commodities but may be less suitable or unsuitable for complex processed foods like dog food.[62] The method has been validated against the known ratio of $FSO_3^-$ to $F^-$ byproducts formed by base hydrolysis of sulfuryl fluoride. Overall, the potentiometric method is rapid, convenient, and economical. The only equipment needed is a pH meter, which is available in portable models. We are currently using the method to monitor $FSO_3^-$ in experimental systems designed to remove $SO_2F_2$ from spent fumigation vapors and convert it to harmless products.[60]

## ■ ASSOCIATED CONTENT

### Ⓢ Supporting Information

The Supporting Information is available free of charge at https://pubs.acs.org/doi/10.1021/acsomega.4c02629.

> Text and tables on purity, recovery in plant tissues, and attempts to determine $KFSO_3$ by ion chromatography. Figures on spectra of food extracts, calibration curves of $FSO_3^-$ vs $NO_3^-$, and electrode response effects with respect to cations and persulfate ions (PDF)

## ■ AUTHOR INFORMATION

### Corresponding Author

Joseph J Pignatello − The Connecticut Agricultural Experiment Station, New Haven, Connecticut 06511, United States; ⦿ orcid.org/0000-0002-2772-5250; Email: joseph.pignatello@ct.gov

### Authors

Zhihao Chen − The Connecticut Agricultural Experiment Station, New Haven, Connecticut 06511, United States; School of Environmental Science and Engineering, East Campus of Sun Yat-sen University, Guangzhou 510330, China

Chengjin Wang − The Connecticut Agricultural Experiment Station, New Haven, Connecticut 06511, United States; Department of Civil Engineering, University of Manitoba, Winnipeg, Manitoba R3T 5 V6, Canada

Complete contact information is available at:
https://pubs.acs.org/10.1021/acsomega.4c02629

### Notes

The authors declare no competing financial interest.

## ■ ACKNOWLEDGMENTS

## ■ REFERENCES

(1) Gillespie, R. J. Fluorosulfuric acid and related superacid media. Acc. Chem. Res. 1968, 1, 202−209.

(2) Jache, A. W. Fluorosulfuric Acid, Its Salts, and Derivatives. Adv. Inorg. Chem. Radiochem. 1974, 16, 177−200.

(3) Bartmann, K.; Mootz, D. Structures of two strong broensted acids: (I) fluorosulfuric acid and (II) trifluoromethanesulfonic acid. Acta Crystallogr., Sect. C: Cryst. Struct. Commun. 1990, 46, 319−320.

(4) Engelbrecht, A. Fluorosulfuric acid as a reaction medium and fluorinating agent in inorganic chemistry. Angew. Chem., Int. Ed. 1965, 4, 641−645.

(5) Revathi, L.; Ravindar, L.; Leng, J.; Rakesh, K. P.; Qin, H. L. Synthesis and chemical transformations of fluorosulfates. Asian J. Org. Chem. 2018, 7, 662−682.

(6) Krespan, C. G.; Dixon, D. A. Fluorosulfonation. Insertion of sulfur trioxide into allylic carbon-fluorine bonds. J. Org. Chem. 1986, 51, 4460−4466.

(7) Smart, B. E. A novel reaction of sulfur trioxide with fluoro olefins. J. Org. Chem. 1976, 41, 2353−2354.

(8) Wei, M. J.; Liang, D. C.; Cao, X. H.; Luo, W. J.; Ma, G. J.; Liu, Z. Y.; Li, L. A broad-spectrum catalytic amidation of sulfonyl fluorides and fluorosulfates. Angew. Chem., Int. Ed. 2021, 133, 7473−7480.

(9) Luy, J. N.; Tonner, R. Complementary base lowers the barrier in SuFEx click chemistry for primary amine nucleophiles. ACS Omega 2020, 5, 31432−31439.

(10) Dong, J.; Krasnova, L.; Finn, M. G.; Sharpless, K. B. Sulfur (VI) fluoride exchange (SuFEx): Another good reaction for click chemistry. Angew. Chem., Int. Ed. 2014, 53, 9430−9448.

(11) Qin, H. L.; Zheng, Q.; Bare, G. A.; Wu, P.; Sharpless, K. B. A Heck−Matsuda process for the synthesis of β-arylethenesulfonyl fluorides: Selectively addressable bis-electrophiles for SuFEx click chemistry. Angew. Chem., Int. Ed. 2016, 55, 14155−14158.

(12) Lee, C.; Cook, A. J.; Elisabeth, J. E.; Friede, N. C.; Sammis, G. M.; Ball, N. D. The emerging applications of sulfur (VI) fluorides in catalysis. ACS Catal. 2021, 11, 6578−6589.

(13) Ball, N. D.; In Emerging Fluorinated Motifs: synthesis, Properties, and Applications, Vol. 2.; Properties and Applications of Sulfur (VI) Fluorides; Wiley-VCH Verlag GmbH & Co. KGaA: 2020; pp. 621671.

(14) Deng, X. Y.; Zhu, X. H. "Recent Advances of S−18F Radiochemistry for Positron Emission Tomography". ACS Omega 2023, 8, 37720−37730.

(15) Wang, N. X.; Yang, B.; Fu, C. Y.; Zhu, H.; Zheng, F.; Kobayashi, T.; Liu, J.; Li, S. S.; Ma, C.; Wang, P. G.; et al. Genetically encoding fluorosulfate-L-tyrosine to react with lysine, histidine, and tyrosine via SuFEx in proteins in vivo. J. Am. Chem. Soc. 2018, 140, 4995−4999.

(16) Cao, A.; Guo, M. X.; Yan, D. D.; Mao, L. G.; Wang, Q. X.; Li, Y.; Duan, X. Y.; Wang, P. S. Evaluation of sulfuryl fluoride as a soil fumigant in China. Pest Manag. Sci. 2014, 70, 219−227.

(17) Grice, J. D.; Gault, R. A.; Chao, G. Y. Reederite-(Y), a new sodium rare-earth carbonate mineral with a unique fluorosulfate anion. Am. Mineral. 1995, 80, 1059−1064.

(18) U.S. EPA; RED (Reregistration Eligibility Document) Facts Sulfuryl Fluoride.; Office of Prevention. In Pesticides And Toxic Substances, EPA; 1993, Vol. 9. (H-7508W). EPA-738-F-93−012

(19) Nie, Y.; Liang, X. J.; Ji, J. B.; Lu, M. Z.; Yu, F. W.; Gu, D. Y.; Xie, Q. L.; Min, M. Harmless treatment of sulfuryl fluoride by chemical absorption. Environ. Eng. Sci. 2015, 32, 789−795.

(20) Meikle, R. W. Fumigant decomposition, fate of sulfuryl fluoride in wheat flour. J. Agr. Food Chem. 1964, 12, 464−467.

(21) Scheffrahn, R. H.; Hsu, R. C.; Osbrink, W. L. A.; Su, N. Y. Fluoride and sulfate residues in foods fumigated with sulfuryl fluoride. J. Agr. Food Chem. 1989, 37, 203−206.

(22) Derrick, M. R.; Burgess, H. D.; Baker, M. T.; Binnie, N. E. Sulfuryl fluoride (Vikane): A review of its use as a fumigant. J. Am. Inst. Conserv. 1990, 29, 77−90.

(23) Hwaidi, M.; Collins, P. J.; Sissons, M.; Pavic, H.; Nayak, M. K. Sorption and desorption of sulfuryl fluoride by wheat, flour and semolina. J. Stored Prod. Res. 2015, 62, 65−73.

(24) Gressent, A.; Rigby, M.; Ganesan, A. L.; Prinn, R. G.; Manning, A. J.; Mühle, J.; Salameh, P. K.; Krummel, P. B.; Fraser, P. J.; Steele, L. P.; et al. Growing atmospheric emissions of sulfuryl fluoride. *J. Geophys. Res.: Atmos.* **2021**, *126*, No. e2020JD034327.

(25) Mühle, J.; Huang, J.; Weiss, R. F.; Prinn, R. G.; Miller, B. R.; Salameh, P. K.; Harth, C. M.; Fraser, P. J.; Porter, L. W.; Greally, B. R. et al. Sulfuryl fluoride in the global atmosphere. *J. Geophys. Res.: Atmos.* **2009**, *114*. .

(26) Friedemann, A. E. R.; Andernach, L.; Jungnickel, H.; Borchmann, D. W.; Baltaci, D.; Laux, P.; Schulz, H.; Luch, A. Phosphine fumigation - Time dependent changes in the volatile profile of table grapes. *J. Hazard. Mater.* **2020**, *393*, 122480.

(27) Hasan, M. M.; Aikins, M. J.; Schilling, M. W.; Phillips, T. W. Sulfuryl fluoride as a methyl bromide alternative for fumigation of Necrobia rufipes (Coleoptera: Cleridae) and Tyrophagus putrescentiae (Sarcoptiformes: Acaridae), major pests of animal-based stored products. *J. Stored. Prod. Res.* **2021**, *91*, 101769.

(28) Sriranjini, V. R.; Rajendran, S. Sorption of sulfuryl fluoride by food commodities. *Pest Manag. Sci.* **2008**, *64*, 873−879.

(29) Meikle, R. W.; Stewart, D. Structural fumigants, the residue potential of sulfuryl fluoride, methyl bromide, and methanesulfonyl fluoride in structural fumigations. *J. Agric. Food Chem.* **1962**, *10*, 393−397.

(30) Erickson, B. E. Fumigant under scrutiny for greenhouse gas emissions. *C&EN* **2022**, *100*, 17.

(31) Evans, J.; Getz, C.; Sellen, J.; 2022/10/27. *Petition to Regulate Sulfuryl Fluoride to Reduce the Use of the High Global Warning Potential Pesticide-A Legal Petition.*

(32) Papadimitriou, V. C.; Portmann, R. W.; Fahey, D. W.; Mühle, J.; Weiss, R. F.; Burkholder, J. B. Experimental and theoretical study of the atmospheric chemistry and global warming potential of $SO_2F_2$. *J. Phys. Chem. A* **2008**, *112*, 12657−12666.

(33) Nie, Y.; Zheng, Q. F.; Liang, X. J.; Gu, D. Y.; Lu, M. Z.; Min, M.; Ji, J. B. Decomposition treatment of $SO_2F_2$ using packed bed DBD plasma followed by chemical absorption. *Environ. Sci. Technol.* **2013**, *47*, 7934−7939.

(34) Tsai, W. T. Environmental and health risks of sulfuryl fluoride, a fumigant replacement for methyl bromide. *J. Environ. Sci. Health, Part C* **2010**, *28*, 125−145.

(35) Dong, Q. X.; Lewis, C. M.; Koshlukova, S.; California Department of Pesticide Regulation Memorandum. In *Establishing Sulfuryl Fluoride Uncertainty Factors for Acute and Short-term Exposures*; Department of Pesticide Regulation, 2017.

(36) Zou, H. L.; Chen, P. P.; Peng, C.; Liang, C. D.; *Lithium ion battery, battery module, battery pack and power consuming device*, Contemporary Amperex Technology CO, 2023.

(37) Jones, M. M.; Lockhart, W. L. Kinetics of decomposition of the fluorosulphate ion in aqueous solution. *J. Inorg. Nucl. Chem.* **1968**, *30*, 1237−1243.

(38) Lawrance, G. A. Coordinated trifluoromethanesulfonate and fluorosulfate. *Chem. Rev.* **1986**, *86*, 17−33.

(39) Michałowski, T.; Malinowski, P. J.; Grochala, W. Synthesis, crystal structures, and selected properties of metal fluorosulfates(VI). *J. Fluor. Chem.* **2016**, *189*, 102−118.

(40) Alleyne, C. S.; Thompson, R. C. Coordinating Properties of the fluorosulfate ion. Tetrakis (pyridine) complexes of zinc (II), copper (II), and nickel (II) fluorosulfates. *Can. J. Chem.* **1974**, *52*, 3218−3228.

(41) Kodani, S. D.; Biochemical toxicology of fluorosulfate, an intermediary metabolite of the fumigant sulfuryl fluoride. In *Disseration*; Spring: University of California, Berkeley, 2012.

(42) U.S. EPA Reviewer; *Data Evaluation Record of Sulfuryl Fluoride/078003: Neurotoxicity and Toxicokinetics − Rat*; EPA, 2015.

(43) Arnold, M. A.; Meyerhoff, M. E. Ion-selective electrodes. *Anal. Chem.* **1984**, *56*, 20−48.

(44) Fakih, I.; Durnan, O.; Mahvash, F.; Napal, I.; Centeno, A.; Zurutuza, A.; Yargeau, V.; Szkopek, T. Selective ion sensing with high resolution large area graphene field effect transistor arrays. *Nat. Commun.* **2020**, *11* (1), 3226.

(45) Hasan, N.; Kansakar, U.; Sherer, E.; DeCoster, M. A.; Radadia, A. D. Ion-selective membrane-coated graphene−hexagonal boron nitride heterostructures for field-effect ion sensing. *ACS Omega* **2021**, *6*, 30281−30291.

(46) Buck, R. P.; Lindner, E. Recommendations for nomenclature of ionselective electrodes (IUPAC Recommendations 1994). *Pure Appl. Chem.* **1994**, *66*, 2527−2536.

(47) Wang, A. L.; Jiang, Y.; Yan, Y. Q.; Bu, L. J.; Wei, Z. S.; Spinney, R.; Dionysiou, D. D.; Xiao, R. Y. Mechanistic and quantitative profiling of electro-Fenton process for wastewater treatment. *Water Res.* **2023**, *235*, 119838.

(48) Bailey, P. L., 2nd. ed. *Analysis with Ion Selective Electrodes*. Heyden & Son Ltd,: London, 1976.

(49) Chen, X. V.; Mousavi, M. P. S.; Bühlmann, P. Fluorous-phase ion-selective pH electrodes: Electrode body and ionophore optimization for measurements in the physiological pH range. *ACS Omega* **2020**, *5*, 13621−13629.

(50) Dura, B.; Choi, J. Y.; Zhang, K.; Damsky, W.; Thakral, D.; Bosenberg, M.; Craft, J.; Fan, R. scFTD-seq: Freeze-thaw lysis based, portable approach toward highly distributed single-cell 3′ mRNA profiling. *Nucleic Acids Res.* **2019**, *47*, No. e16.

(51) Chen, Z. H.; Li, J. Y.; Chen, M. Q.; Koh, K. Y.; Du, Z. R.; Gin, K. Y.; He, Y. L.; Ong, C. N.; Chen, J. P. Microcystis aeruginosa removal by peroxides of hydrogen peroxide, peroxy monosulfate and peroxydisulfate without additional activators. *Water Res.* **2021**, *201*, 117263.

(52) Cady, G. H.; Misra, S. Hydrolysis of sulfuryl fluoride. *Inorg. Chem.* **1974**, *13*, 837−841.

(53) Causey, A. G.; Hill, H. M.; Phillips, L. J. Evaluation of criteria for the acceptance of bioanalytical data. *J. Pharm. Biomed. Anal.* **1990**, *8* (8−12), 625−628.

(54) Mohamed, G. G.; El-Shahat, M. F.; Al-Sabagh, A. M.; Migahed, M. A.; Ali, T. A. Septonex−tetraphenylborate screen-printed ion selective electrode for the potentiometric determination of Septonex in pharmaceutical preparations. *Anal* **2011**, *136*, 1488−1495.

(55) Paul, A.; Nair, R. R.; Chatterjee, P. B.; Srivastava, D. N. Fabrication of a Cu (II)-Selective electrode in the polyvinyl chloride matrix utilizing mechanochemically synthesized rhodamine 6g as an ionophore. *ACS Omega* **2018**, *3*, 16230−16237.

(56) Xu, K. B.; Li, Y.; Li, M. Potentiometric phosphate ion sensor based on electrochemical modified tungsten electrode. *ACS Omega* **2021**, *6*, 13795−13801.

(57) Tratnyek, P. G.; Grundl, T. J.; Haderlein, S. B.; *Aquatic redox chemistry*, American Chemical Society, 2011.

(58) Sugiyama, S.; Yokoyama, M.; Ishizuka, H.; Sotowa, K. I.; Tomida, T.; Shigemoto, N. Removal of aqueous ammonium with magnesium phosphates obtained from the ammonium-elimination of magnesium ammonium phosphate. *J. Colloid Interface Sci.* **2005**, *292*, 133−138.

(59) Lee, S. I.; Weon, S. Y.; Lee, C. W.; Koopman, B. Removal of nitrogen and phosphate from wastewater by addition of bittern. *Chemosphere* **2003**, *51*, 265−271.

(60) Pignatello, J. J.; Wang, C. J.; Chen, Z. H.Method for Scrubbing Sulfuryl Fluoride from A Fluid 18/703097US, **2024**

(61) Austel, N.; Schubert, J.; Gadau, S.; Jungnickel, H.; Budnik, L. T.; Luch, A. Influence of fumigants on sunflower seeds: Characteristics of fumigant desorption and changes in volatile profiles. *J. Hazard. Mater.* **2017**, *337*, 138−147.

(62) Raditic, D. M.; Remillard, R. L.; Tater, K. C. ELISA testing for common food antigens in four dry dog foods used in dietary elimination trials. *J. Anim. Physiol. Anim. Nutr.* **2011**, *95*, 90−97.